

A Machine Learning Approach to Model the Received Signal in Molecular Communications

H. Birkan Yilmaz, Changmin Lee, Yae Jee Cho, and Chan-Byoung Chae

School of Integrated Technology, Institute of Convergence Technology, Yonsei University, Korea.

Email: {birkan.yilmaz, cm.lee, yjenncho, cbchae}@yonsei.ac.kr

Abstract—A molecular communication channel is determined by the received signal, which forms the basis for studies that are focusing on modulation, receiver design, capacity, and coding. Therefore, it is crucial to model the number of received molecules until time t . Received signal is modeled analytically when the transmitter is a point and the receiver is an absorbing sphere. Modeling the diffusion-based molecular communication channel with the first-hitting process (i.e., with an absorbing receiver) is an open issue when the transmitter is a reflecting spherical body. In this paper, we utilize the artificial neural networks technique to model the received signal for a spherical transmitter and a perfectly absorbing receiver (i.e., first-hitting process). The proposed technique may be utilized in other studies that assume a spherical transmitter instead of a point transmitter.

I. INTRODUCTION

Nanotechnology is a promising technology that has numerous potential applications [1], [2]. One of its innovative approaches is to utilize collaborative behavior amongst small entities. To enable the revolutionary possibilities of nanotechnology, it is important to possess the capacity to communicate at the nano- and micro-scale [3]. As a possible means to communicate at such a small scale, researchers have proposed molecular communication via diffusion (MCvD) [4]. In an MCvD system, molecules (emitted by a transmitter) propagate through the environment until they arrive at the receiver node, which constitute the received signal.

One of the main challenges in molecular communication (MC) is to develop valid models for representing the received signal in different environments and conditions. Some of the MCvD models in the literature, assume that whenever a molecule hits the receiver it is removed from the environment [5]–[7]. This phenomenon is modeled by the first-passage process. In this model, each molecule can contribute to the received signal only once. In [5], the authors presented the analytical model for the received signal in a 1-dimensional (1D) environment while considering the first-passage process. In [7], the authors presented the expected cumulative number of received molecules when the transmitter is a point source and the receiver is an absorbing spherical node in a 3D medium. In [8], the authors analytically modeled the received signal and derived the expected cumulative number of received molecules when the receptor effect was added to the system presented in [7].

On the other hand, some of the MCvD models ignore the first-passage process, allowing molecules to pass through the receiver node surface/boundary with no interaction between

the environment and the receiver [9]–[11]. In such models, the molecules are allowed to contribute to the signal multiple times, as they can pass in and out of the receiver node surface multiple times. In [11], the authors considered such a spherical transmitter that does not reflect the molecules, only the initial emission points are selected randomly at the transmitter and molecules can pass through the transmitter node surface with no interaction. The main difference between our work and [11] is the reflection property of the transmitter node in our study, i.e., molecules cannot pass through the transmitter node's boundary after they are emitted.

Both of the MCvD physical layer models are summarized and presented in [3]. In [12], it is claimed that the first-passage process is observed in nature more frequently than the passive receiver process. The absorbing spherical receiver model with a reflecting spherical transmitter is similar to the MC systems in nature [12]. Both channel models (i.e., the received signal for the first-passage process and passive receiver) have a common hurdle for the communication engineering: heavy tail distribution of the received signal, which causes inter-symbol-interference (ISI). In literature, plenty of techniques are proposed to eliminate the severe effects of ISI by utilizing specialized modulations [13], error correcting codes [14]–[16], and enzymes [17], [18]. In these studies, analytical models are used for the derivations, which indicates the importance of modeling the received signal in different environments.

Modeling the MCvD channel with the first-passage process is an open issue for a spherical transmitter that emits molecules from a single point and reflects the emitted molecules as in the case of hormonal secretion in the synapses and pancreatic β -cell islets [17]. In general, emitter cells do not have receptors of emitted molecules at the emission site, otherwise the transmitter would directly absorb the self emitted molecules. To the best of our knowledge, an analytical formulation does not exist in the literature for the spherical perfectly absorbing receiver when the transmitter is a reflecting spherical body. In this paper, we propose a machine learning based approach to model the diffusion channel for a more realistic topology [19]. The proposed model function is inspired by our previous work in [7], while it has additional model parameters that act as compensation parameters. Moreover, we show that these model parameters can be learned by an artificial neural network (ANN) and the trained ANN can estimate the model parameters by using only

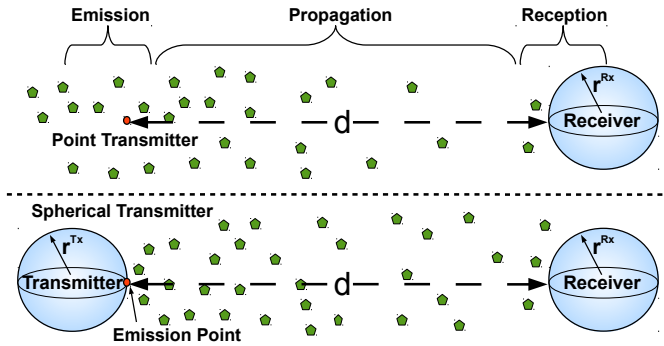


Fig. 1. System model of MCvD with point and spherical transmitter cases. In the point transmitter case, molecules are free to go in the opposite direction.

the given system parameters as input.

II. SYSTEM MODEL

We consider an MCvD system with one transmitter and receiver pair in a fluid environment. Fig. 1 shows two different cases for MCvD—point and spherical transmitters. In general, the point transmitter case is studied in the literature [7], [8], [10]. The point transmitter assumption is reasonable for some applications. However the transmitter node has a body in general and the transmitter does not react to the molecules from itself [12]. In this paper, we model the MCvD channel with a perfectly absorbing receiver without the point transmitter assumption.

As shown in Fig. 1, emitted molecules diffuse in the 3D environment, which is characterized by the diffusion coefficient D . At the receiver side, the radius of the receiver is denoted by r^{Rx} and the received signal consists of the time histogram of hitting molecules. When we have a point transmitter, molecules are able to travel in the opposite direction of the receiver more freely. In the spherical transmitter case, however, molecules are obstructed and reflected by the transmitter of radius r^{Tx} . Hence, the received signals of these two cases are expected to differ.

A. MCvD with a Point Transmitter

The received signal is modeled analytically for the point transmitter and the spherical perfectly absorbing receiver case. The diffusion process basically models the average movement of particles in the concentration gradient. In [7], the solution to the differential equation system that defines the system is presented and analyzed from the perspective of channel characteristics. After finding the reaction rate, the formula for the fraction of molecules that hit the receiver by the time t is presented as follows:

$$F_{\text{hit}}^{\text{3D}}(t) = \frac{r^{\text{Rx}}}{d+r^{\text{Rx}}} \operatorname{erfc}\left(\frac{d}{\sqrt{4Dt}}\right) \quad (1)$$

where d and $\operatorname{erfc}(\cdot)$ represent the distance and complementary error function. For the spherical transmitter case, it is more complex to derive the formulation of the number of received molecules due to the lack of circular symmetry.

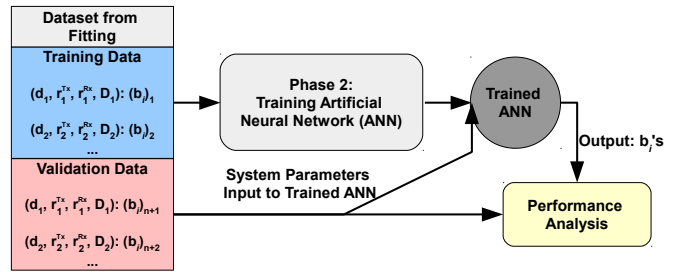


Fig. 2. Flowchart of the proposed technique. Phase 1 deals with fitting model parameters by utilizing the simulator output. Phase 2 deals with training the ANN on the training dataset that is obtained from Phase 1. Dataset from Phase 1 consists of input-output pairs where input is $(d, r^{\text{Tx}}, r^{\text{Rx}}, D)$ and the output consists of the model parameters (i.e., b_i 's).

B. MCvD with a Spherical Transmitter

Modeling the received signal analytically for a spherical transmitter is an open issue when the receiver is a perfectly absorbing spherical receiver in a 3D environment. The main difference and hurdle stem from the lack of circular symmetry in differential equations system. For the spherical transmitter case, molecules are biased towards going in the direction of the receiver due to the obstructing body of the transmitter node. Therefore, each of the molecules is expected to have a higher probability of hitting the receiver.

Hurdles caused by a spherical transmitter steered us to simulate the MCvD with a spherical transmitter and to analyze the patterns so as to grasp the underlying dynamics. We ran extensive simulations with many parameters. The cumulative number of received molecules exhibits a similar behavior to the point transmitter case with a small perturbation that depends on the system parameters.

III. PROPOSED TECHNIQUE FOR CHANNEL MODELING

As noted above, the main challenge in MCvD is to develop valid models for representing the received signal in different environments and conditions. When the transmitter has a spherical body, we propose to model the received signal by parameterizing (1) and learning the patterns behind the model parameters. For the fitting phase, we use a similar approach to [20] by introducing compensation parameters.

The proposed technique has two main phases: fitting the model parameters constitutes phase one (i.e., forming the input-output dataset for phase two) and learning the patterns in the input-output dataset constitutes phase two. After the learning phase, the output of the algorithm is a trained ANN for future predictions on unexplored input (i.e., other combinations of system parameters that are not considered during the training phase). A representative scheme of the proposed technique is depicted in Fig. 2.

A. Model Function and Fitting

We propose two different model functions for fitting the simulation data and name them as the *primitive model* and

enhanced model. We use only a scaling factor for the primitive model, which is represented as follows:

$$F_{\text{hit}}^{3\text{D}}(t, b_1) = b_1 \frac{r^{\text{Rx}}}{d+r^{\text{Rx}}} \operatorname{erfc}\left(\frac{d}{\sqrt{4Dt}}\right) \quad (2)$$

where b_1 represents the model fitting parameter. For the enhanced model, we also parametrize the components related to D and t , which is shown as follows:

$$F_{\text{hit}}^{3\text{D}}(t, b_1, b_2, b_3) = b_1 \frac{r^{\text{Rx}}}{d+r^{\text{Rx}}} \operatorname{erfc}\left(\frac{d}{(\sqrt{4D})^{b_2} t^{b_3}}\right) \quad (3)$$

where b_1 , b_2 , and b_3 are model fitting parameters. These model fitting parameters are introduced for fitting simulation data to model functions. When the transmitter is a reflecting sphere we expect more molecules at the receiver and earlier arrivals of molecules. Therefore, we add scaling and time related model fitting parameters.

To find the model parameters corresponding to the system parameters, we use nonlinear least squares curve fitting technique. We considering N time instances to formulate the fitting model parameters problem with m parameters as follows:

$$\arg \min_{b_1, \dots, b_m} \sum_{k=1}^N \left(F_{\text{hit}}^{3\text{D}}(t_k, b_1, \dots, b_m) - S_{\text{hit}}^{3\text{D}}(t_k) \right)^2 \quad (4)$$

where $S_{\text{hit}}^{3\text{D}}(t)$ corresponds to the mean simulation data that is representing the ratio of hitting molecules until time t , which is evaluated over simulation realizations.

The output of the curve fitting process consists of the model parameters (i.e., b_1 for primitive model and $b_1 \sim b_3$ for the enhanced model). Hence, we obtain model parameters for each simulation case, which forms the dataset of the next phase. This dataset structure is depicted in Fig. 2, which contains the system parameters and b_i 's from curve fitting.

B. Learning Model Parameters

In this paper, we utilize a machine-learning technique to model the received signal in MCvD with a spherical transmitter. One of the popular machine-learning techniques is artificial neural networks. They have simple neuron-like nodes with thresholds and connections with weights. Basically, the thresholds and the weights are adjusted until the desired output is observed for the given inputs.

The dataset from the curve fitting phase is divided into two disjointed subsets as training and validation datasets. Training data is utilized for training the ANN for getting the desired output for given inputs. Bayesian regularization backpropagation technique is used for the ANN training that updates the weights and bias values according to Levenberg-Marquardt optimization. Bayesian regularization minimizes a combination of squared errors and weights of the ANN to determine the ANN parameters that generalize the pattern in the input-output pairs. We utilize the trained ANN¹ to estimate

¹The trained ANN and the data can be downloaded from Matlab fileexchange (public domain) <http://tinyurl.com/ANN-for-S2S-MCvD>

TABLE I
RANGE OF PARAMETERS USED IN THE EXPERIMENTS

| Parameter | Value |
|---|--|
| Number of emitted molecules | 3 000 |
| Simulation duration (t_{end}) | 1 s |
| Simulation time step | 5×10^{-5} s |
| Replication | 500 |
| TDS Distances (d) | {2, 4, 6, 8, 10} μm |
| VDS Distances (d) | {3, 5, 7, 9, 11} μm |
| TDS Transmitter radii (r^{Tx}) | {5, 7.5, 10} μm |
| VDS Transmitter radii (r^{Tx}) | {4, 6, 8} μm |
| TDS Diffusion coefficients (D) | {50, 75, 100} $\mu\text{m}^2/\text{s}$ |
| VDS Diffusion coefficients (D) | {60, 70, 80} $\mu\text{m}^2/\text{s}$ |
| TDS Receiver radii (r^{Rx}) | {5, 7.5, 10} μm |
| VDS Receiver radii (r^{Rx}) | {4, 6, 8} μm |

the channel parameters for different cases. Note that the curve-fitting technique requires simulation data for training the ANN but the trained ANN does not require any simulation data, i.e., required inputs are the system parameters such as d , r^{Tx} , D , and r^{Rx} . After training the ANN we do not need any simulations for obtaining the channel model function parameters; we will be able to get the channel model function parameters for unknown cases by utilizing the trained ANN. Simulation and fitting are used to produce the training dataset (TDS) for training the ANN. Details of the dataset will be given in the following section.

IV. RESULTS AND ANALYSIS

A. Performance Metrics and Parameters

For the performance metrics, we use root mean squared error (RMSE) with respect to simulation data in terms of number of received molecules to get insight about the performance of the ANN technique. First, we give the received signal and signal-to-inter-symbol-interference ratio (SISIR) plots for the example cases. We then present the average RMSE over different cases.

Common system parameters for simulation, training (TDS), and validation (VDS) datasets are presented in Table I. From the given datasets, each of the VDS and TDS have $5 \times 3 \times 3 \times 3 = 135$ different cases, making a total of 270 cases. Each simulation case is replicated 500 times to estimate the mean received signal at the receiver side (i.e., $F_{\text{hit}}^{3\text{D}}(t)$).

What is of prime interest for modeling an MCvD channel is to model, as noted above, the received signal (i.e., the number of hitting molecules until time t). To model the received signal, we utilize curve-fitting and artificial neural network techniques. In the performance figures, we cannot present all 135 cases, but we offer some example scenarios and average RMSE plots.

B. Received Signal Analysis

In Fig. 3, the received signal is plotted for simulation data, curve-fitting, and ANN techniques. Note that the ANN technique requires no simulation data, while the curve-fitting method does. After training an ANN, we estimated channel

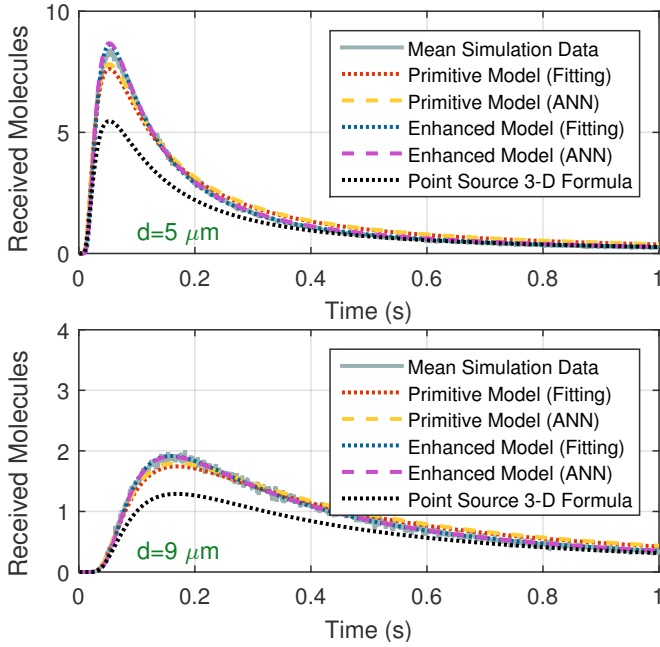


Fig. 3. Received signal plots for $r^{\text{Tx}} = 4 \mu\text{m}$, $r^{\text{Rx}} = 8 \mu\text{m}$, $D = 80 \mu\text{m}^2/\text{s}$, and $d = \{5, 9\} \mu\text{m}$ with time resolution of 1 ms.

model parameters for the validation data by giving only the system parameters as input. For the *primitive model* that is given in (2), a single channel model parameter was estimated. On the other hand, for the *enhanced model* that is given in (3), three channel model parameters were estimated.

It can be clearly seen that the *enhanced model* fits the simulation data better than does the *primitive model*. At the peak and the tail part of the received signal, we observe that the *enhanced model* outperforms the *primitive model* and the point transmitter formulation given in (1). The second observation suggests that, with increased distance, the estimation performance of the received signal is improved. This observation will also be supported by SISIR and RMSE plots in Figs. 4 and 5. The diminishing effect of spherical transmitter may be the reason behind this observation. Another observation is that the trained ANNs generalize the fitted model parameters well.

C. SISIR Analysis

Interference is the primary impairment in MC due to the heavy tail structure of the received signal [17]. Hence, modeling the inter-symbol-interference (ISI) is at a crucial importance and in literature finite number of ISI slots are considered. Therefore, we also analyze SISIR metric (with a sufficiently large t_{end} that depends on the system parameters), which is formulated as:

$$\text{SISIR}(t) = \frac{F_{\text{hit}}^{3\text{D}}(t)}{F_{\text{hit}}^{3\text{D}}(t_{\text{end}}) - F_{\text{hit}}^{3\text{D}}(t)} \quad (5)$$

where we can also substitute $F_{\text{hit}}^{3\text{D}}(t)$ with the channel model functions given in (2) and (3). This metric basically represents

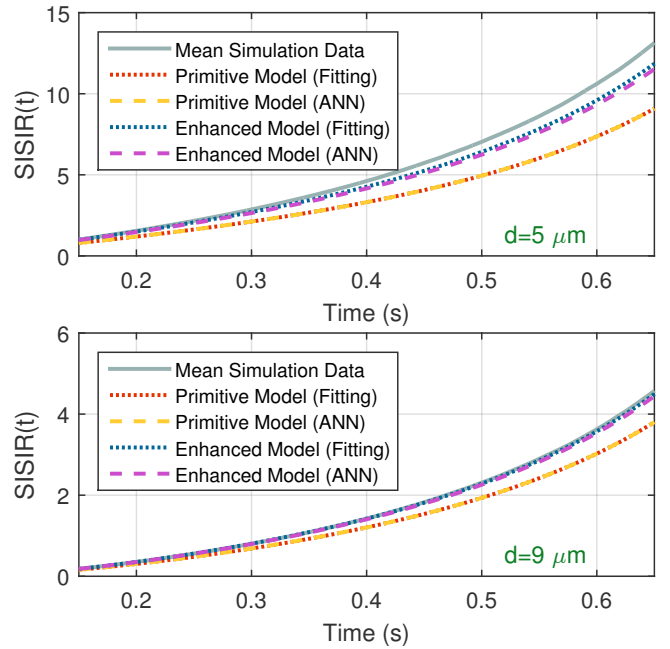


Fig. 4. SISIR plots for $r^{\text{Tx}} = 4 \mu\text{m}$, $r^{\text{Rx}} = 8 \mu\text{m}$, $D = 80 \mu\text{m}^2/\text{s}$, and $d = \{5, 9\} \mu\text{m}$ with time resolution of 1 ms.

the ratio of the cumulative number of received molecules until time t and the number of ISI molecules that could not be received in the current symbol duration. SISIR plots are important since they show the performance of modeling the ratio of desired signal and ISI.

In Fig. 4, SISIR is plotted for the simulation data, curve-fitting, and ANN techniques. The *enhanced model* estimates the received signal better than the *primitive model*. Moreover, the longer the distance the better the channel parameter estimation performance. For $d = 9 \mu\text{m}$ case, the *enhanced model* is very close to the simulation data. However, the *primitive model* with one scaling factor does not adequately model the simulation data. Again, we see that the trained ANN generalizes the fitting method well for both of the cases (i.e., fitting and ANN curves are overlapping for both models).

D. RMSE Analysis

To better understand the performance of the estimation technique, we evaluated the mean RMSE of cases with respect to (wrt) simulation data in terms of the number of received molecules until time t . For RMSE analysis, we grouped results with respect to distance and r^{Rx} so that each group is the average of nine cases.

In Fig. 5, the RMSEs of the channel parameter estimation methods are presented for ANNs with *primitive* and *enhanced* models. The first observation from both subfigures suggests that the estimation performance gets better with increasing distance. Moreover, the RMSE of the *enhanced model* is significantly lower than that of the *primitive model*. Note that the ANN technique requires no simulation data, utilizing only the system parameters as input to estimate the channel

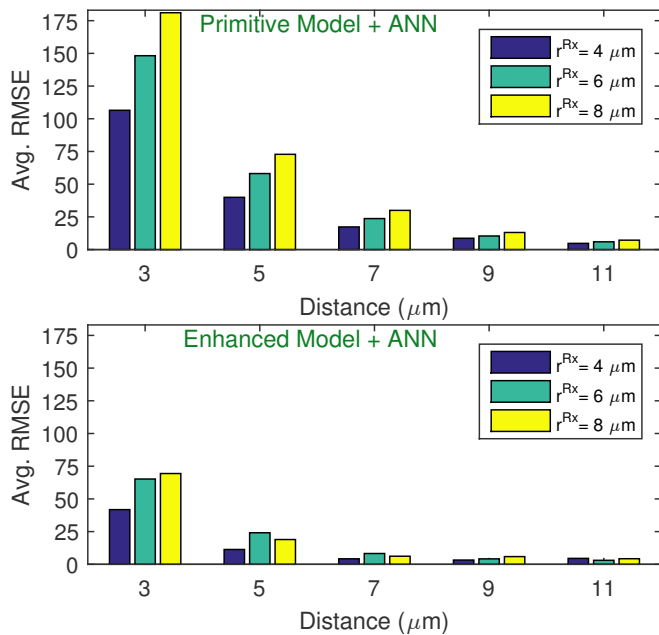


Fig. 5. Average RMSE plots of ANN estimation.

parameters. The *primitive model* scales the formulation of point transmitter case and the larger r^{Rx} case deviates more from the point transmitter case, as the probability rises of receiving obstructed and reflected molecules. Therefore, for the *primitive model*, performance of the estimation of the received signal is better in terms of RMSE for smaller r^{Rx} .

V. CONCLUSION

In this work, we developed a novel technique to model the received signal in MCvD with a spherical transmitter. In the literature, a point transmitter is assumed for the tractability of the mathematical derivations in a first-passage process framework. Approaching the problem from a unique perspective, we utilized an artificial neural network technique and a model function for the number of received molecules. After training an ANN, we were able to ask the ANN to estimate the channel model parameters for different system setups. Our proposed technique has promising results for modeling the number of received molecules until time t . We observed that the proposed technique models the received signal and SISIR more effectively for longer distances. The proposed technique may be utilized to model an MCvD channel in other studies that assumes a spherical transmitter instead of a point transmitter.

ACKNOWLEDGMENT

This research has been supported by the MSIP (Ministry of Science, ICT and Future Planning), Korea, under the ‘‘ICT Consilience Creative Program’’ (IITP-R0346-16-1008) supervised by the IITP (Institute for Information & Communications Technology Promotion) and by the Basic Science Research Program (2014R1A1A1002186) funded by

the MSIP, Korea, through the National Research Foundation of Korea.

REFERENCES

- [1] N. Farsad, H. B. Yilmaz, A. W. Eckford, C.-B. Chae, and W. Guo, ‘‘A comprehensive survey of recent advancements in molecular communication,’’ *IEEE Commun. Surveys Tuts.*, vol. 18, no. 3, pp. 1887–1919, 2016.
- [2] I. F. Akyildiz, J. M. Jornet, and M. Pierobon, ‘‘Nanonetworks: a new frontier in communications,’’ *Commun. ACM*, vol. 54, no. 11, pp. 84–89, Nov. 2011.
- [3] W. Guo, T. Asyhari, N. Farsad, H. B. Yilmaz, B. Li, A. Eckford, and C.-B. Chae, ‘‘Molecular communications: channel model and physical layer techniques,’’ *IEEE Wireless Commun. Mag.*, vol. 23, no. 4, pp. 120–127, 2016.
- [4] S. Hiyama, Y. Moritani, T. Suda, R. Egashira, A. Enomoto, M. Moore, and T. Nakano, ‘‘Molecular communication,’’ in *Proc. NSTI Nanotechnol. Conf. (NanoTech)*, 2005, pp. 391–394.
- [5] K. V. Srinivas, A. W. Eckford, and R. S. Adve, ‘‘Molecular communication in fluid media: The additive inverse Gaussian noise channel,’’ *IEEE Trans. Inf. Theory*, vol. 58, no. 7, pp. 4678–4692, Jul. 2012.
- [6] T. Nakano, Y. Okaie, and J.-Q. Liu, ‘‘Channel model and capacity analysis of molecular communication with Brownian motion,’’ *IEEE Commun. Lett.*, vol. 16, no. 6, pp. 797–800, Jun. 2012.
- [7] H. B. Yilmaz, A. C. Heren, T. Tugcu, and C.-B. Chae, ‘‘Three-dimensional channel characteristics for molecular communications with an absorbing receiver,’’ *IEEE Commun. Lett.*, vol. 18, no. 6, pp. 929–932, Jun. 2014.
- [8] A. Akkaya, H. B. Yilmaz, C.-B. Chae, and T. Tugcu, ‘‘Effect of receptor density and size on signal reception in molecular communication via diffusion with an absorbing receiver,’’ *IEEE Commun. Lett.*, vol. 19, no. 2, pp. 155–158, Feb. 2015.
- [9] D. Kilinc and O. B. Akan, ‘‘Receiver design for molecular communication,’’ *IEEE J. Sel. Areas Commun.*, vol. 31, no. 12, pp. 705–714, 2013.
- [10] M. Pierobon and I. F. Akyildiz, ‘‘A physical end-to-end model for molecular communication in nanonetworks,’’ *IEEE J. Sel. Areas Commun.*, vol. 28, no. 4, pp. 602–611, 2010.
- [11] A. Noel, D. Makrakis, and A. Hafid, ‘‘Channel impulse responses in diffusive molecular communication with spherical transmitters,’’ *arXiv preprint arXiv:1604.04684*, 2016.
- [12] P. Cuatrecasas, ‘‘Membrane receptors,’’ *Annu. Rev. Biochem.*, vol. 43, no. 1, pp. 169–214, Jul. 1974.
- [13] N.-R. Kim, A. W. Eckford, and C.-B. Chae, ‘‘Symbol interval optimization for molecular communication with drift,’’ *IEEE Trans. NanoBiosci.*, vol. 13, no. 3, pp. 223–229, Sep. 2014.
- [14] M. S. Leeson and M. D. Higgins, ‘‘Forward error correction for molecular communications,’’ *Elsevier Nano Commun. Netw.*, vol. 3, no. 3, pp. 161–167, Sep. 2012.
- [15] M. U. Mahfuz, D. Makrakis, and H. T. Mouftah, ‘‘Performance analysis of convolutional coding techniques in diffusion-based concentration-encoded PAM molecular communication systems,’’ *Springer Bio-NanoSci.*, vol. 3, no. 3, pp. 270–284, Sep. 2013.
- [16] P.-J. Shih, C.-H. Lee, P.-C. Yeh, and K.-C. Chen, ‘‘Channel codes for reliability enhancement in molecular communication,’’ *IEEE J. Sel. Areas Commun.*, vol. 31, no. 12, pp. 857–867, Dec. 2013.
- [17] M. Ş. Kuran, H. B. Yilmaz, and T. Tugcu, ‘‘A tunnel-based approach for signal shaping in molecular communication,’’ in *Proc. IEEE Int. Conf. on Commun. (ICC)*, 2013, pp. 776–781.
- [18] A. Noel, K. C. Cheung, and R. Schober, ‘‘A unifying model for external noise sources and ISI in diffusive molecular communication,’’ *IEEE J. Sel. Areas Commun.*, vol. 32, no. 12, pp. 2330–2343, 2014.
- [19] A. Patnaik, D. E. Anagnostou, R. K. Mishra, J. Lyke *et al.*, ‘‘Applications of neural networks in wireless communications,’’ *IEEE Antennas Propag. Mag.*, vol. 46, no. 3, pp. 130–137, 2004.
- [20] N. Farsad, N.-R. Kim, A. W. Eckford, and C.-B. Chae, ‘‘Channel and noise models for nonlinear molecular communication systems,’’ *IEEE J. Sel. Areas Commun.*, vol. 32, no. 12, pp. 2392–2401, Dec. 2014.